A novel in-flight thrust modulation technique for SPRM: proof of concept

A novel in-flight thrust modulation technique for SPRM: proof of concept

A M Abdelraouf [1], O K Mahmoud[2] and M A Al-Sanabawy[3]
[1] M.Sc. Student, Rocket Department, Military Technical College, Cairo, Egypt
[2] Dr. Eng., Military Technical College, Cairo, Egypt
[3] Assoc. Prof., Military Technical College, Cairo, Egypt

E-mail: eng.ahmed.2147@gmail.com

Abstract. Thrust modulation (termination or reduction) is one of the most sophisticated topics in rocket motors. Thrust termination is employed when combustion must be terminated to ensure proper stage separation, to avoid motor explosion, to attain certain range, or for research purposes. While liquid and hybrid propellant rocket motors have the ability to extinguish thrust, thrust termination in solid propellant rocket motors (SPRMs) need the use of specialized technology. In-flight thrust termination of (SPRMs) can be achieved by sudden and sufficient increase in throat area. Increasing throat area causes high depressurization rate which consequently leads to extinguishing the rocket motor. In contrast, in-flight thrust reduction can be theoretically attained either by reducing chamber pressure to a new equilibrium level or by reducing the divergent section length. The objective of the present paper is to prove the concept of using Linear Shaped Charge (LSC) for thrust modulation; a technique novel to SPRM applications. Thrust termination concept is proved via a set of static firing tests on a standard test motor. In addition, a mathematical model is developed to predict the drop in thrust due to cutting the nozzle at any arbitrary location. The model is validated by comparing with published experiments for thrust termination and reduction. A parametric study is conducted based on model results. It is confirmed that by cutting the nozzle along its divergent section, thrust reduction less than 20% can be attained. Further reduction can be achieved by cutting the nozzle along its convergent section.

1. Introduction

A rocket motor is basically an energy conversion device. By oxidizing the fuel, hot gases that are produced subsequently accelerate into the nozzle, giving the rocket motor thrust, thus mechanical work is done. Conventional rocket propellants include solid, liquid and hybrid ones. Solid propellant rocket motors (SPRMs) are preferred over other conventional chemical rocket engines when high reliability, quick operational readiness, and convenient storage are required. The most significant disadvantages of SPRMs are that: (1) they are extremely difficult to extinguish (terminate thrust), necessitating the use of specific technology, and (2) they produce non-controllable thrust unless prior sophisticated design concepts are imposed. In fact, thrust termination is one of the most complicated issues. It is used in situations when stopping the functioning of a rocket engine prior to burnout is desired. To name a few situations: (1) once the vehicle has reached the required velocity (to obtain a pre-set velocity for a ballistic missile or an exact orbit for a satellite); (2) a safety precaution is to be taken when it appears that a flight test vehicle may unexpectedly fly out of the safe limitations of a flight test range facility; (3) to avoid stage collisions during

a multistage vehicle separation maneuver, which may involve a thrust reversal; (4) when a partially-burnt motor is to be studied for research and development purposes [1]; and (5) to protect the motor when unexpected increase in pressure may cause explosion hazard [2].

Mechanism of combustion and, hence, mechanism of thrust termination are dependent on chemical composition of solid propellant being either the homogeneous double-based propellant (DB) or the heterogeneous composite propellant (CP). The combustion flame structure of DB propellants is homogeneous along the burning direction. Experiments show that there are four separate zones, as shown in Figure1: the burning surface (known as foam zone), the fizz zone, the dark zone, and the flame zone [3]. Nitroglycerine (NG) and nitrocellulose (NC) decompose in the foam zone. The dark zone, which can range in size from 0.1 to 2 cm, exists between the fizz zone and the flame zone. The dark zone reduces as pressure rises, and it practically vanishes at high pressures of roughly 7 MPa. The principal processes that occur in the flame zone are the oxidation of CO and H_2 to CO_2 and H_2O, respectively, and the reduction of NO to N_2 occurs around 3000 K, indicating a significant rise in temperature. If the dark zone is not excessively thick, the propellant surface receives a significant amount of heat, which makes extinguishment more difficult [4].

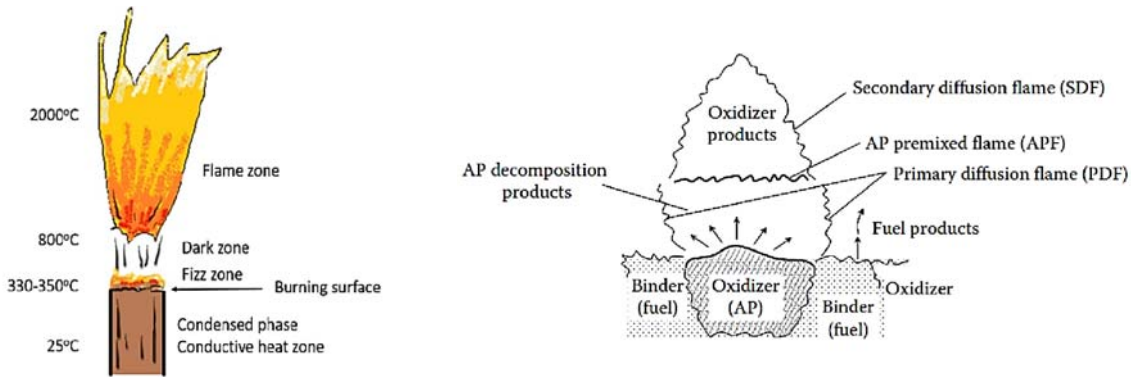

(a) Case of DB propellants (b) Case of composite propellants

Figure1. Flame structure and combustion mechanisms

In contrast, the heterogeneous physical structure of CP yields a heterogeneous combustion wave structure. When the propellant surface is heated, the Ammonium Perchlorate (AP) crystal in the fuel decomposes into oxidizing gases, while the fuel is pyrolyzed to generate hydrocarbon vapors. The chamber pressure rises, and the fuel products become more difficult to spread and mix with the oxidizer stream. As a result, two reaction pathways become competitive as shown in Figure1b: (1) Oxidizing products and ammonia from AP decomposition, and (2) fuel (binder) products and AP oxidizing products. Because chemical reactions occur more quickly under higher pressures, oxidizer products interact with ammonia to create a premixed flame before binder products can mix with the oxidizer products. A Primary Diffusion Flame (PDF) is created, when a fraction of the oxidizing products comes into contact with the fuel pyrolysis products. Because this flame is oxidizer-rich, a large portion of oxidizer products (approximately 30%) remains unburned during AP premixed flame production. Unburned oxidizer products combine with the fuel-rich pyrolysis products, so that a Secondary Diffusion Flame (SDF) is created, with a maximum temperature of 3200 K. As the chamber pressure rises, the thickness of the combustion zone shrinks [3, 5].

As they differ in combustion mechanisms, DB propellant is easier to extinguish than composite propellant because of the presence of a dark zone which keeps the flame away from the propellant surface. In contrast for composite propellant, the flame zone is in direct contact to the surface. Furthermore, the inclusion of Al particles in the combined fuel reduces the pressure gradient required for extinction while allowing re-ignition. Solid propellants can be extinguished via two different techniques namely, fluid quenching and rapid depressurization. Occasionally, fluid quenching technique to achieve thrust termination of solid

propellants was implemented to quench the propellant by injecting liquid into the motor [6, 7, 8, 9]. This technique implies using a pressurized tank with pressure higher than that of combustion which adds a heavy load on the motor assembly. So, such technique can only be implemented in static fire tests while it is inappropriate for flight applications.
In the other technique, (also known as dp/dt quenching) the chamber pressure is abruptly reduced below Propellant Deflagration Limit (PDL) determined experimentally by Crawford bomb [10]. If the pressure is gradually reduced, the gaseous and solid phase processes will adjust, and the instantaneous burning velocity will achieve the value of steady burning at the given pressure. In contrast, if dp/dt is high enough, not all parameters will be able to quickly adapt. Consequently, there will be a delay between heat transfer in the solid, which corresponds to high pressure, and that in the gas, which corresponds to low pressure, leading to a discontinuity in the temperature derivative near the surface. Studies have identified the dp/dt pressure gradient required for extinguishing [1, 10]. It has been shown also that the composition of the propellant has an impact on the pressure gradient. For instance, Aluminum has been demonstrated through experiments to minimize the required pressure gradient, although it may also allow for re-ignition [10]. Rapid depressurization was implemented where mechanisms to open extra ports or to increase the throat area that achieve rapid pressure drop were applied [11, 12, 13, 14]. Both mechanisms necessitate the use of explosive devices namely, explosive bolts, and pyrotechnic valves to achieve the instantaneous depressurization [15, 16].

In contrast, thrust reduction is solely achieved by prior design of a stepped- (dual-) thrust motor. Using a single motor, this boost-sustain mode of motor operation is implemented via using one grain of sophisticated design or using a complicated variable nozzle [3, 17]. It can be also implemented using two grains of different compositions, or different designs [1]. In all cases, the motor nozzle remains intact. One grain of simple design placed in a motor with simple fixed nozzle would only produce monotonic thrust. The thrust relation is expressed as

$$F = \dot{m}W_e + (P_e - P_a)A_e \tag{1}$$

where F =Thrust, $\dot{m}$,= mass flow rate of gases, W_e,= exit velocity, P_e = exit pressure, P_a= atmospheric pressure, and A_e = nozzle exit area. Thus, the thrust produced from a single grain can be reduced if the nozzle length is reduced by cutting away a part of it. Values of parameters in the above equation would change depending on whether nozzle is cut upstream or downstream of the throat. In both cases, the surrounding atmospheric pressure, P_a , remains unchanged, nozzle exit area, A_e, and exit pressure, P_e, increase, while exit velocity, W_e, decreases. Mass flow rate of gases, $\dot{m}$, decreases only if the nozzle is cut upstream of nozzle throat. In both cases, thrust is reduced and a dual boost-sustain thrust mode can be achieved. Despite its apparent simplicity and feasibility, the concept of in-flight thrust reduction via nozzle length reduction has not been explored in the open literature.

Linear Shaped Charge (LSC) is a technique that is commonly implemented in cases where reliable and instantaneous separation is sought. It has found wide range of applications such as launch vehicle stage separation, aircraft emergency escape, and payload fairing separation [18]. Shaped charges are used not only in military engineering but also in civil engineering. For example, a shaped charge can be used to create a long crack in oil exploration, to cut pipes underwater, to cut a large or thick metal structure that is difficult to cut by common methods, and to break a rock or concrete block [19]. LSC was implemented as a thrust termination system in which two ports were opened at the head end of the rocket motor [20]. Using LSC as a thrust reduction technique was not proposed in the open literature so far. In addition, the concept of thrust reduction via nozzle cutting using an LSC deserves preliminary assessment leading to practical validation. Based on the previously reported applications, LSC is believed to offer a more reliable, more economic, and less sophisticated means for thrust termination and reduction.

The present paper reports the results of a recent research work in which LSC is used to terminate and reduce thrust of a solid propellant test rocket motor. The goal of the paper is to provide a proof-of-concept for LSC implementation in real flights. The paper also aims at developing a mathematical model for the steady state response of the motor due to the sudden change of nozzle critical or exit areas via LSC implementation. The model can serve as a design tool to define the change needed for a given thrust reduction or for complete thrust termination. The remainder of the paper is organized as follows. Aspects of the test motor examined and methodology of study are discussed first. Next, the main results are presented and discussed. The paper wraps up with key conclusions and recommendations.

2. Case study and methodology

2.1. Test motor

The case study motor is a thick-walled static test motor, Figure 2. The motor is packed with one single perforated grain with a length of 0.277 m, a perforation diameter of 0.083 m, and a web thickness of 0.0385 m. Pressure inside combustion chamber is controlled by nozzle throat diameter. Two throat diameters are adopted here namely, 0.018 m and 0.021 m. while nozzle exit diameter is 0.0475 m to yield two different chamber pressures.

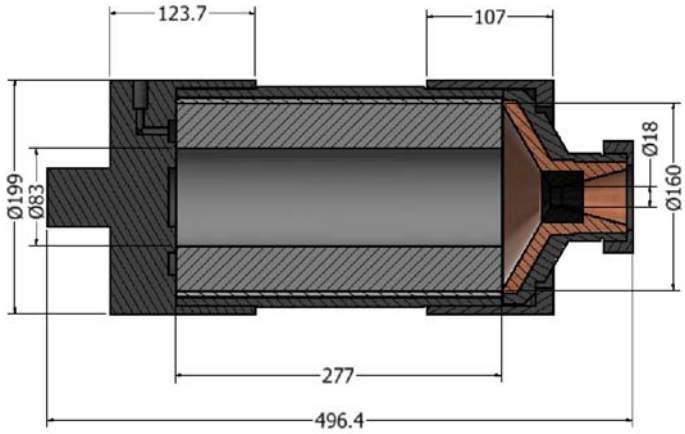

Figure 2. Thick-walled test motor

The grain is made of a typical composite solid propellant consisting of 69% AP, 17% Al powder, 10.08% HTPB, 0.53% HMDI, 0.37% MAPO and 3.02% DOZ. Ballistic and thermochemical characteristics of the propellant are listed in Table 1 below. (The burning law is expressed as: $r_0 = aP_c^n$).

Table 1. Propellant characteristics

Parameter	Value
Gas constant for combustion products, R	318 J/(kg K)
Ratio of specific heats of combustion gases γ	1.24
Adiabatic flame temperature of combustion gases	2800 K
Propellant specific mass ρ_p	1750 kg/m^3
Burning rate constant a	0.0001725
Burning rate pressure index n	0.237
Thermal diffusivity α_p	2.2E-7 m^2/s

Thrust termination and reduction technique used in this study is rapid depressurization via suddenly changing the critical/ exit area of the case study motor. To prove the concept, the whole nozzle is made to separate from the motor by cutting away the cylindrical section at the motor end upstream of the nozzle using a Linear Shaped Charge (LSC). A spacer is used to retain the cylinder containing the propellant inside the motor casing after cutting the nozzle away such that the propellant is prevented from leaving the motor. An LSC is typically composed of an explosive charge packed inside a metallic sheath in the form of linear tubes of specially-profiled cross-section, Figure 3a. Explosives available for use in LSC include RDX, CH6, HMX, PBXNS, and HNS while sheath material include Lead, Copper, Aluminum, and Silver [18]. Selection of sheath material is mainly dependent on the material to be cut and the required depth according to the following relation [21]:

$$P = L \times \sqrt{\frac{\rho_j}{\rho_t}} \tag{2}$$

where P is the depth of penetration while ρ_j and ρ_t are densities of sheath and target metal materials, respectively. L is the stand-off distance, Figure 3a.

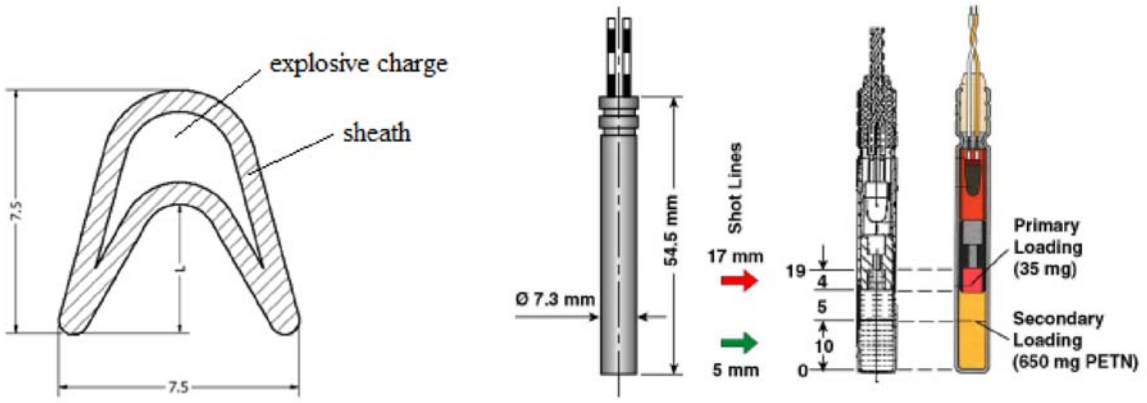

(a) LSC (b) detonator No.8

Figure 3. Construction and dimensions of LSC and detonator

Depending on the material and thickness of flange used, an LSC with RDX as explosive and lead as sheath material with dimensions shown in Figure 3a is adopted. Initiating the LSC is achieved using detonator No.8 which is an aluminum container carrying 35 mg of Lead azide as a primary explosive and 650 mg of PETN as a secondary explosive with main dimensions as shown in Figure 3b [22]. Eventually, the configuration of assembled test motor along with thrust termination mechanism is illustrated in Figure 4.

2.2. Test facility and experiment setup

A pressure transducer is fitted to the test motor; Model: AOV/MOV; Type: full bridge strain gauge, with accuracy 0.5 % of full scale; Range of pressure: about 200 bars, Frequency: larger than 100 kHz; and Output pressure: 2mv/v. During pressure measurement test, the test motor is fitted to a sliding-bed static test stand. Signals from pressure transducers are treated by a data acquisition system, Figure 5.

Two signals are sent from the control room to the test motor: ignition signal and LSC detonation signal. As soon as the first signal is delivered to the igniter, the solid propellant starts to burn. Next, the second signal is sent to detonator with a lag (nearly midway along motor typical operation time). This signal initiates the LSC, producing an effective cutting jet, and then cut the rear flange to release the nozzle under internal pressure. By utilizing spacer to retain the cylinder containing the propellant inside the motor casing after cutting, the propellant is prevented from leaving the motor.

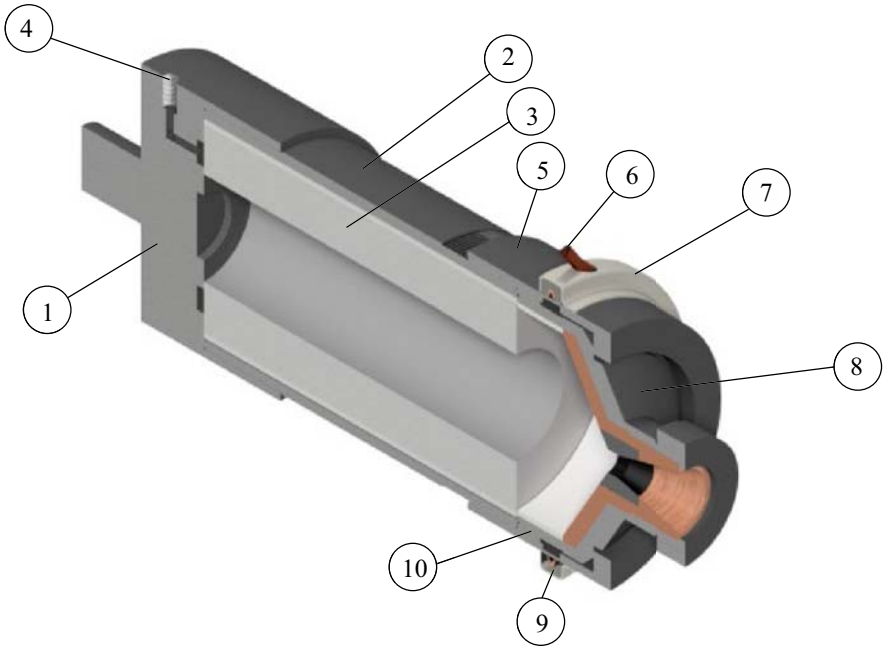

Figure 4. Modified solid propellant rocket motor for thrust termination tests 1- Front cap, 2- Motor case, 3- Solid propellant, 4- Pressure transducer port, 5- Rear flange, 6- LSC, 7- Confinement, 8- Nozzle, 9- Rubber, 10- Spacer

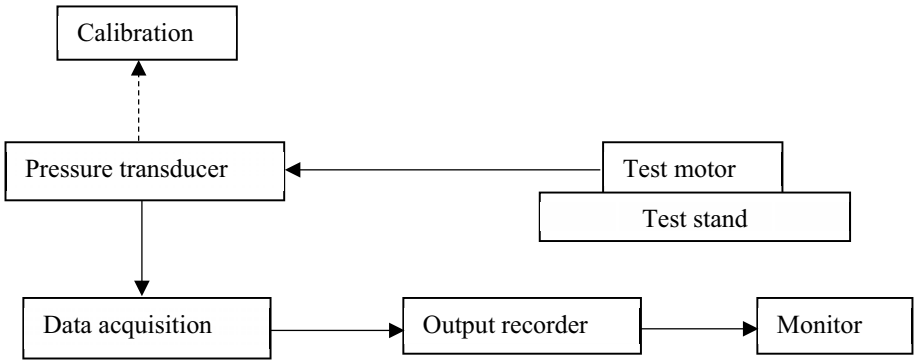

Figure 5. Scheme of complete test facility

2.3. Mathematical modelling of thrust reduction and termination

In order to predict the variation in pressure-time curve due to sudden increase in throat or exit areas of SPRM, a mathematical model is developed based on characteristic properties of the propellant charge in the rocket motor, grain geometry and propellant deflagration pressure limit determined experimentally via Crawford bomb. The core of the mathematical model is the Internal Ballistics Prediction Module (IBPM) developed by the research group. IBPM capability of predicting pressure- and thrust-time profiles has been validated for a variety of SPRMs [23, 24]. The developed mathematical model handles the three different cases namely, Case 1: no cutting of the nozzle; Case 2: the nozzle is cut along its convergent section (for both thrust termination and reduction); and Case 3: the nozzle is cut along its divergent section (for thrust reduction only).

For cases 1 and 3, chamber pressure-time profile does not change since throat area remains unchanged. In contrast, thrust-time profile varies depending on the exit area, A_e according to Equation (1).

Hence, for case 3, only thrust reduction is possible whereas thrust termination cannot be attained. For case 2, both thrust reduction and termination are possible. In this case, the variation in pressure-time profile is depicted using the following equation [25]:

$$\frac{dP_c}{dt} = \frac{\Gamma^2}{V_c}\left(\rho_p C^{*2} A_b a P_c^n - C^* P_c A_t\right) \quad (3)$$

where $\frac{dP_c}{dt}$ is depressurization rate while V_c and P_c are chamber free volume and pressure, respectively. C^*, a ,n, and ρ_p are characteristic velocity, constant of burning, pressure index, and density of propellant respectively. A_t and A_b are throat and burning areas, respectively. The instantaneous burning rate of the solid propellant, r, is then calculated as [11]:

$$r = r_0 \left[1 + \psi\left(\frac{n\,\alpha_p}{P_c\, r_0^2}\right)\frac{dP_c}{dt}\right] \quad (4)$$

where r_0 is the steady propellant burning rate, α_p.is the thermal diffusivity. The constant ψ happens to be very close to unity [3]. Once the instantaneous chamber pressure value is calculated, the motor thrust can be calculated using the isentropic flow relations [26].

Thrust termination occurs when the burning rate r is set to zero, resulting in the critical depressurization rate,$-\frac{dP_c}{dt}$, calculated by [27]:

$$-\frac{dP_c}{dt} = \frac{1}{\psi}\left(\frac{P_c\, r_0^2}{n\,\alpha_p}\right) \quad (5)$$

Hence, pressure-time and thrust-time profiles can be readily calculated. The model checks if the new pressure is smaller than the deflagration pressure, causing full thrust termination. In the opposite case when the pressure is higher than the deflagration pressure, the model checks whether the slope of pressure drop in tail-off phase is higher than the critical one estimated above, causing motor shut off. If not, the burning continues with new equilibrium pressure. In such cases, rather than termination, thrust is reduced to a new equilibrium level that can be used as a boost-sustain dual-thrust profile. Figure 6 shows a flowchart for the mathematical model developed in the present study.

3. Results and discussions

3.1. Experimental thrust termination of static test motor

Figure 7 shows a comparison of the motor chamber pressure-time history for a typical operation with and without throat area increase. Increasing the throat diameter from 0.018 to 0.165 m at 86 bar causes a depressurization fast enough to terminate the thrust after 2.5 sec from ignition signal. The combustion pressure falls to ambient pressure yielding zero thrust. For the sake of confirmation, another thrust termination experiment at operating pressure 56 bar was also conducted in which throat diameter was increased from 0.021 to 0.165 m. Despite that combustion pressure falls to ambient pressure in both experiments, observations with high-speed thermal cameras indicate that there is no full extinguishment of propellant grain and the flame remains until the propellant is completely depleted. This may be explained by the high percentage of aluminum used in this propellant mixture that allows for re-ignition of grain even at very low pressures.

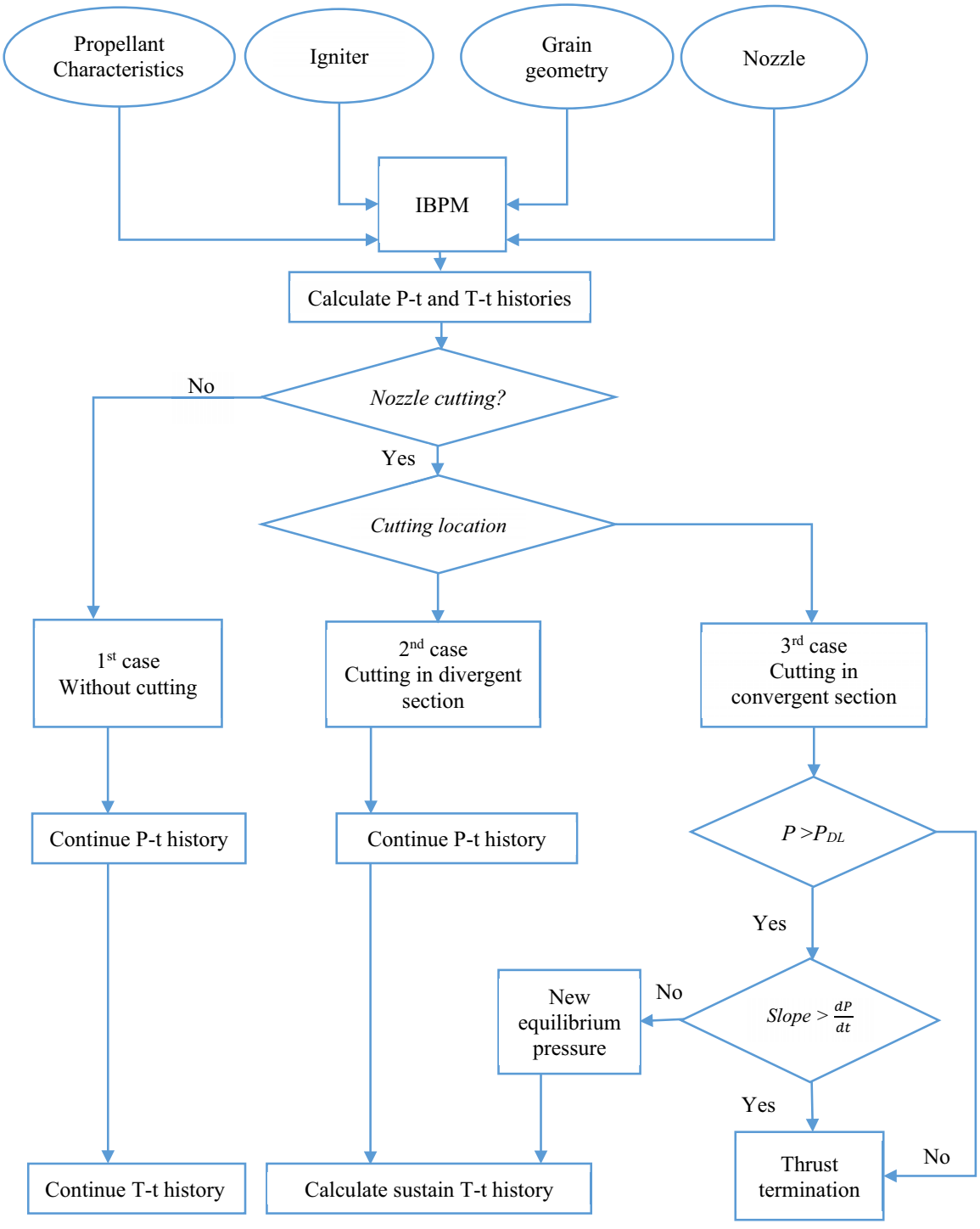

Figure 6. Flow chart of the developed mathematical model

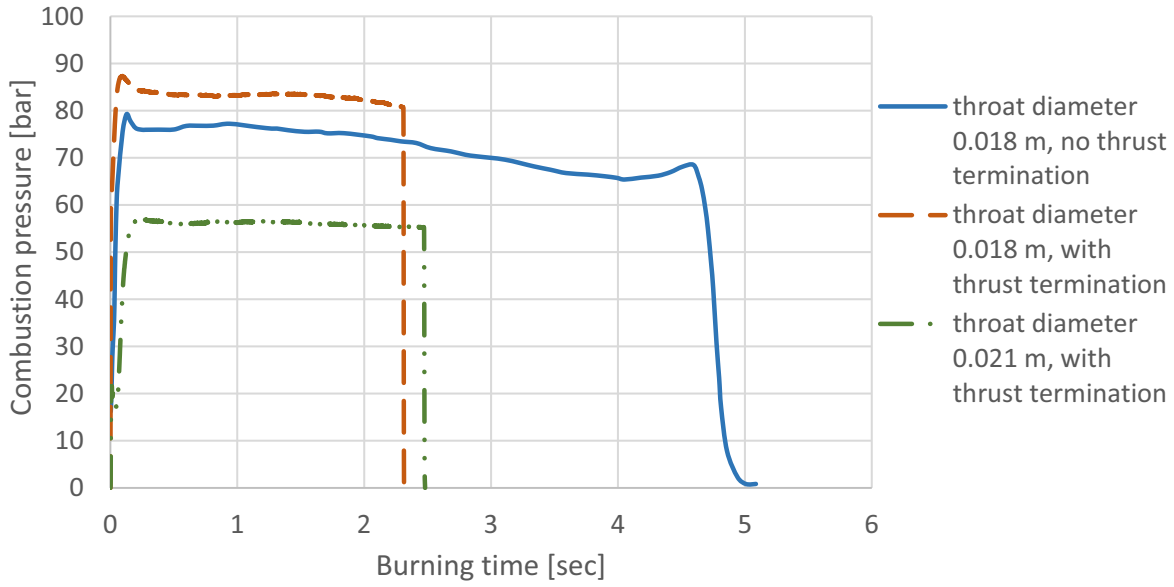

Figure 7. Experimental pressure time curve for thrust termination tests

3.2. Validation of mathematical model

The presented code is validated through comparison with available experimental data by Tahsini and Farshchi [11] for a rocket motor with a cylindrically perforated grain. They used two secondary nozzles (openings) of different sizes at the motor head end to cause thrust termination and reduction via sudden increase in throat area. Values of main parameters of the used motor are listed in Table 2 below. Experimental results of three cases were reported, namely, (1) without opening the secondary nozzles, (2) with opening the smaller secondary nozzle such that the throat area is increased by a factor of 1.77, and (3) with opening the larger secondary nozzle such that the throat area is increased by a factor of 4.69.

Table 2. Experimental data for validation [11]

Parameter	Value
Grain length	0.8 m
Grain perforation diameter	0.1 m
Grain web thickness	0.02 m
Main Nozzle throat diameter	0.06 m
Main Nozzle exit diameter	0.12 m
Gas constant for combustion gases	318 J/(kg K)
Ratio of specific heats of combustion gases	1.21
Adiabatic flame temperature of combustion gases	2800 K
Propellant specific mass	1700 kg/m^3
Burning rate constant	0.005
Burning rate pressure index	0.4

Validation results of the proposed model are shown in the set of figures below in comparison with their reported experimental counterparts. Case 1 shown in Figure 8a is for a motor without opening the secondary nozzle. The motor operates normally as demonstrated by both experimental and model results. In case 2 shown in Figure 8b, the smaller secondary nozzle is opened such that the ratio between the total throat area and main throat area is 2.77. The resulting pressure-time profile indicates a rapid depressurization after the smaller secondary nozzle is opened. However, there is no extinguishment and the motor achieves a new equilibrium at about 18 bar and continues burning until the propellant is completely depleted. In case 3 represented by Figure 8c, opening the larger secondary nozzle with ratio between the total throat area to main throat area of 5.69 leads to occurrence of rapid depressurization leading to full propellant extinguishing. In all cases, the mathematical model shows the same trends of pressure profiles with deviation less than 7.5%. This deviation may be due to mathematical model simplifying assumptions (quasi one-dimensional, isentropic flow of ideal gases with no pressure drop along the nozzle) as well as possible nozzle throat erosion (not reported in [11]).

3.3. Parametric study on impact of cutting location on thrust reduction and termination

The validated mathematical model is employed to calculate and analyze the dependence of pressure and thrust reduction on location of nozzle cutting using the LSC. On the one hand, partially cutting the nozzle away along the convergent section yields a sudden increase in throat area causing both chamber pressure and thrust to drop as confirmed from the above results. The value of throat area enlargement depends on whether it is desired to completely terminate the thrust or to reduce it and the desired boost-sustain thrust ratio (i.e., the new equilibrium pressure). For example, by increasing the throat area by a factor of 2, the mathematical model predicts the pressure profile shown in Figure 9 where the pressure drops by a factor of 0.403. As a consequence, the exhaust velocity shows a dramatic change from supersonic (W_e= 2268 m/s, Mach 3.12) to subsonic (W_e=331 m/s, Mach 0.311), the mass flow rate drops from 1.368 to 0.551 kg/s, while the exit pressure increases from 1.44 to 29.92 bar. Eventually, the thrust drop shown in Figure 9 is attained.

Figure 10 showed the relationship between the pressure drop and the increase in the throat area, which is predicted by a mathematical model. The outcome of this pressure drop depends on the propellant's Pressure Deflagration Limit (PDL). If the new pressure falls below the PDL, the motor will shut off, but if it remains above the PDL, the motor will continue to operate at a lower combustion pressure. The figure also shows the impact on motor thrust. In case of using the nozzle cutting technique as a thrust reduction approach, the new throat area can be decided based on the desired sustain-to-boost thrust ratio.

On the other hand, in the case of partially-cutting the nozzle away along its divergent section using LSC, only thrust is reduced whereas chamber pressure remains unchanged as the throat area remains the same. For instance, for the test case motor used in this study, cutting the nozzle immediately downstream of its throat, i.e., $A_e/A_t = 1$, causes a 22.25% drop in thrust as shown in Figure 11.

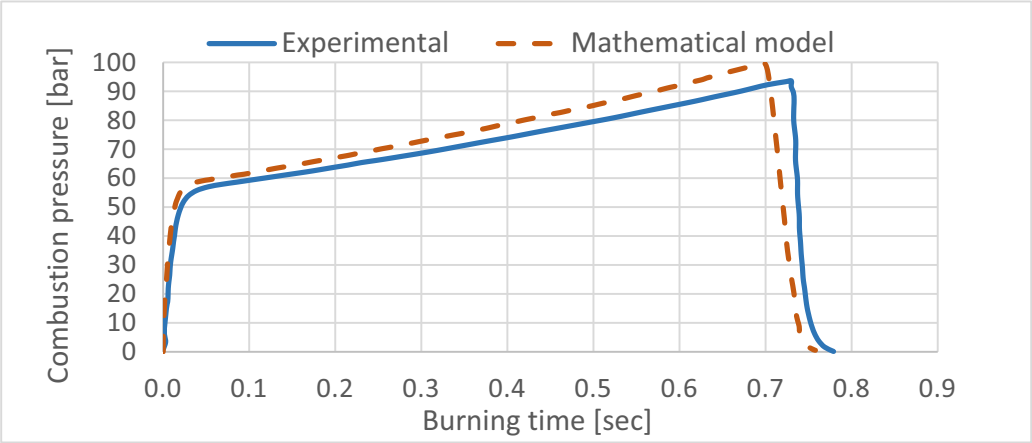

(a) Measured and calculated pressure-time histories for the first case

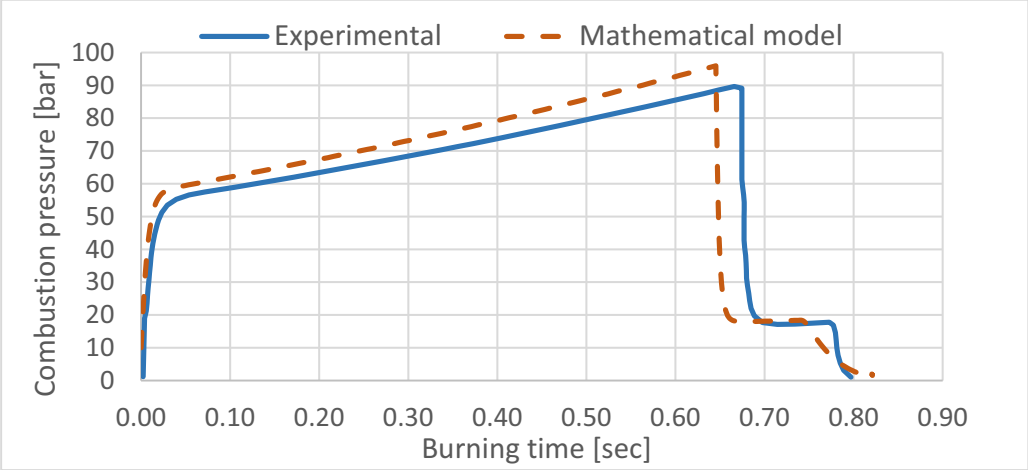

(b) Measured and calculated pressure-time histories for the second case

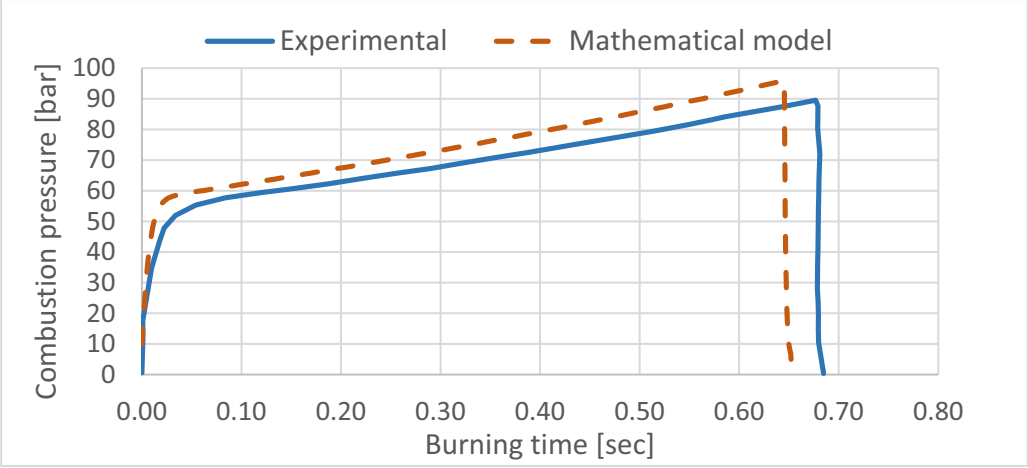

(c) Measured and calculated pressure-time histories for the third case

Figure 8. Results of validation of the proposed mathematical model

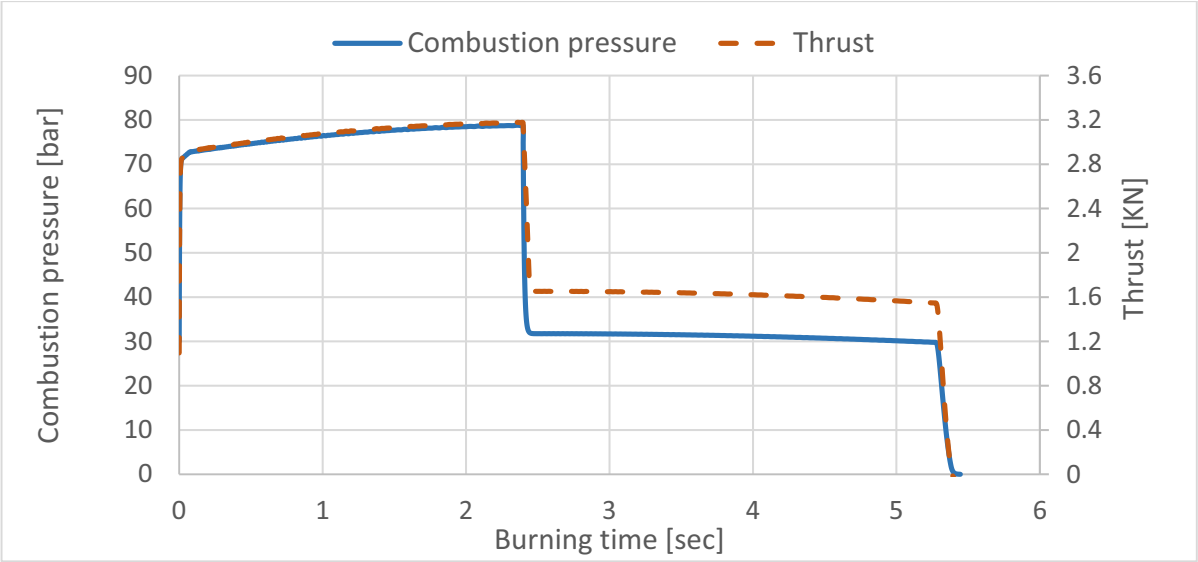

Figure 9. Profiles of pressure and thrust for $A_{t,new}/A_{t,0} = 2$

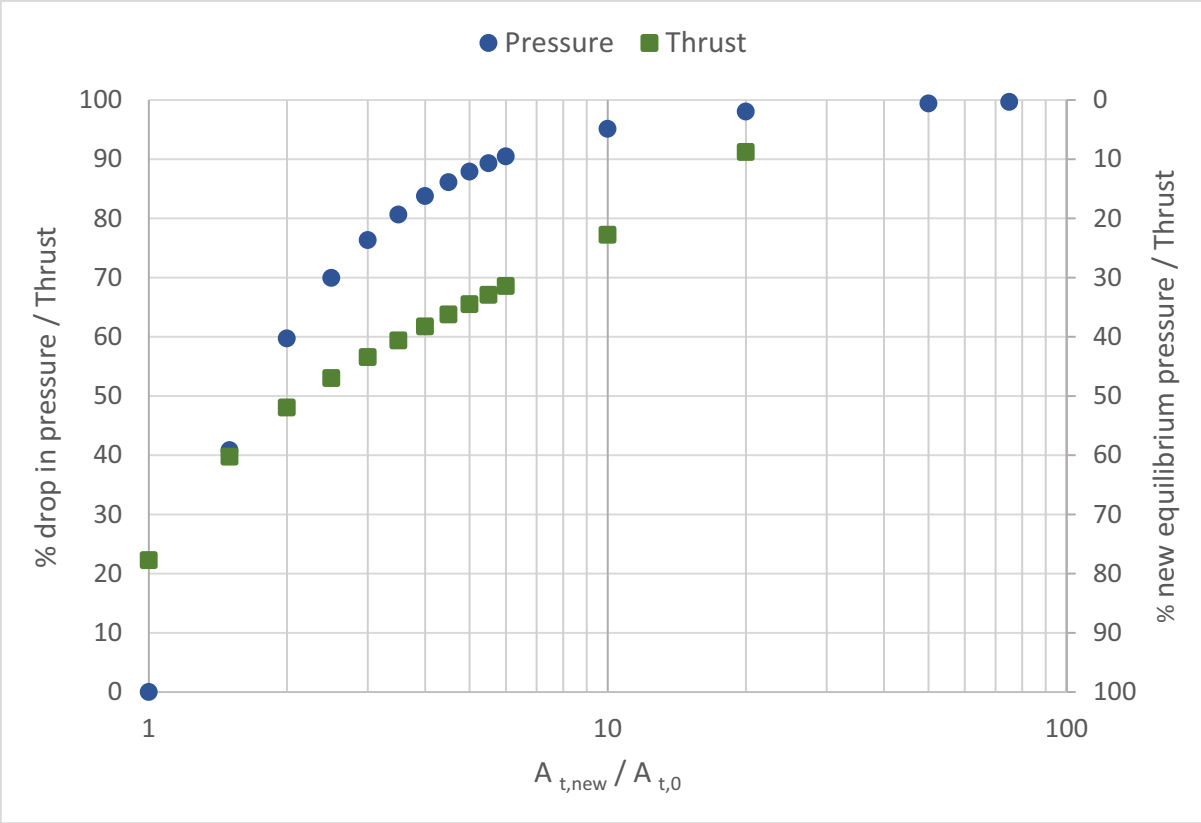

Figure 10. Drop in chamber pressure and motor thrust due to increase in throat area

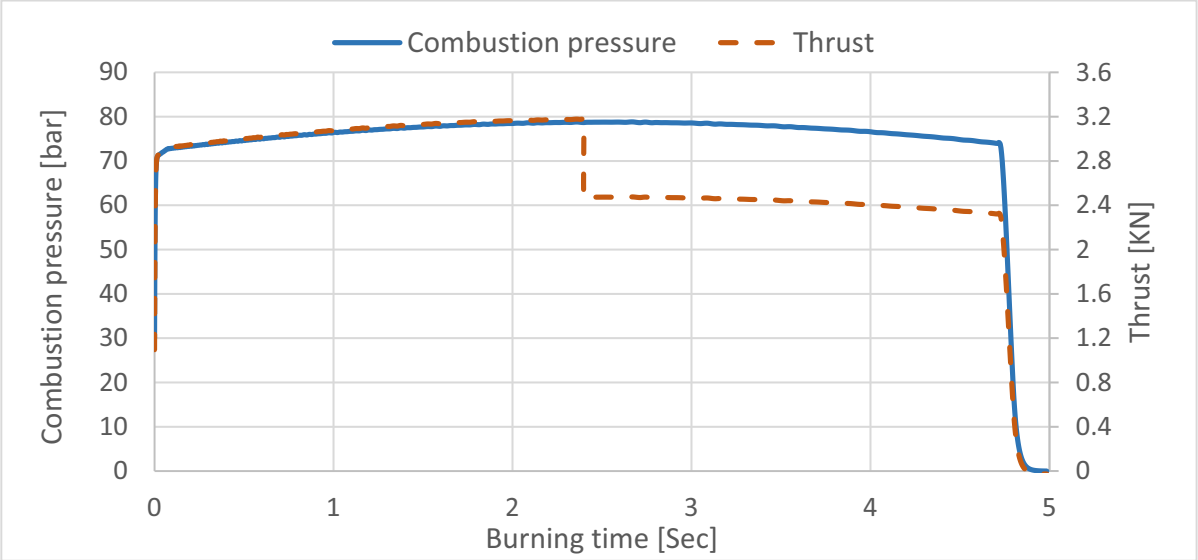

Figure 11. Profiles for pressure and thrust for area ratio for A_e/A_t=1

Figure 12 below shows the dependence of thrust drop due to decrease in the nozzle exit area based on mathematical model prediction. The area ratio of the test motor is 7. The drop on thrust increases as the location on divergent section cutting approaches the throat. Cutting the entire divergent section away yields maximum thrust drop of 22.25% as indicated above in Figure 11.

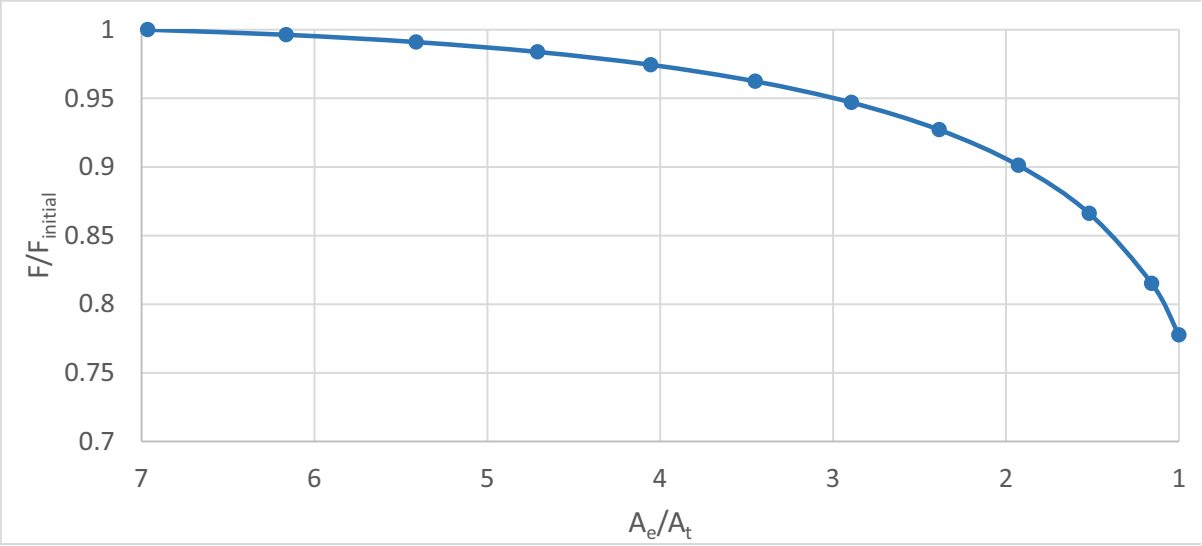

Figure 12. Impact of exit area decrease on thrust reduction

Finally, Figure 13 below summarizes the results of the parametric study by illustrating the impact of nozzle cutting location (normalized with respect to nozzle full length) on sustain-to-boost ratio of the test case motor. A ratio higher than 80% can be achieved by cutting the nozzle along its divergent section. Sustain-to-boost ratios less than 80% can be achieved by cutting along the convergent section. It is important here to indicate that, for the case study in hand, cutting the nozzle such that x/L_{nozzle} is less than 0.17 yields thrust termination rather than reduction as the chamber pressure becomes lower than PDL of the propellant.

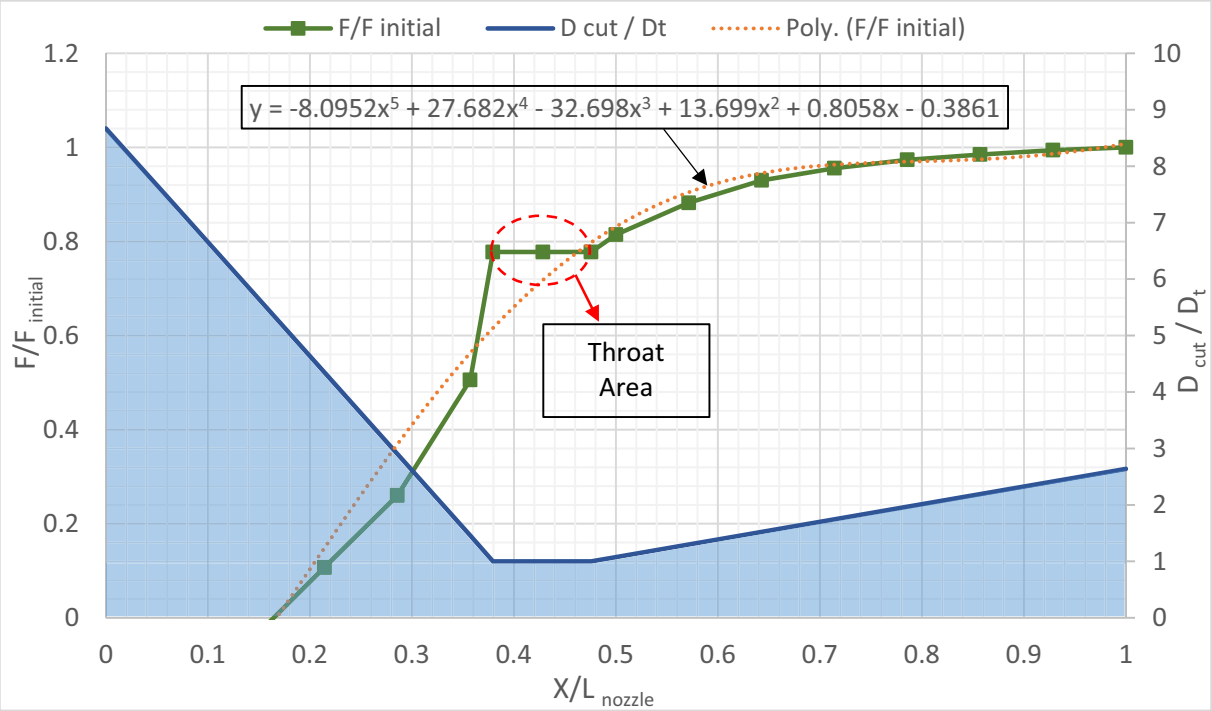

Figure 13. Impact of nozzle cutting location on thrust reduction

4. Conclusion

In-flight thrust termination in solid propellant rocket motor (SPRM) is an extremely sophisticated procedure. It can be achieved by abruptly reducing the chamber pressure below the deflagration limit of the propellant. In contrast, in-flight thrust reduction without prior design of motor and propellant grain is not even possible; presenting one of the SPRM drawbacks. Theoretically though, thrust reduction can be achieved by dropping the chamber pressure to a new equilibrium level or by reducing the nozzle exit area. The goal of the present paper was to prove a novel concept for in-flight thrust termination and reduction by partially cutting the nozzle away. This is attained using a Linear Shaped Charge (LSC) which reliability has been proved in other applications. An SPRM was designed for this goal and a set of static firing tests was performed. The concept of LSC as a reliable thrust termination technique was proved. In addition, a mathematical model was developed based on internal ballistics relations to estimate the change in chamber pressure and motor thrust due to nozzle cutting at different locations along it. The model was validated by comparing its simplified steady-state results with published experimental measurements; a justification for the 7.5% deviation was attempted. A parametric study was conducted based on the mathematical model to illustrate the dependence of pressure and thrust drop on the location along the nozzle at which cutting via LSC can be applied. For the case study motor, it was concluded that a thrust reduction less than 20% can be achieved if the nozzle exit area is reduced by partially cutting it away along the divergent section and the chamber pressure remains unchanged. Higher thrust reduction implies reducing the chamber pressure

and the nozzle should be cut away along its convergent section. However, cutting more than 80% of the nozzle entire length would cause thrust termination rather than reduction.
The developed mathematical model can be further enhanced to increase its accuracy and to predict transient behavior of motor. In addition, the new concept should be proved in real in-flight thrust reduction and termination applications.

References

[1] Sutton G P and Biblarz O 2001 *Rocket Propulsion Elements Seventh Edition* (United States of America.: A Wiley-Interscience publication) chapter 13 pp 526-28.
[2] Kuo K, Mantzaras J and Moreci J 1987 Different Modes of Crack Propagation in Burning Solid Propellants *J. Propulsion* **3** pp 19-25.
[3] Mishra D 2017 *Fundamentals of Rocket Propulsion* (Boca Raton: Taylor & Francis Group) chapter 7 pp 199-203.
[4] Warren L R, Wang Z, Pulham C R and Morrison C A 2020 A Review of the Catalytic Effects of Lead-Based Ballistic Modifiers on the Combustion Chemistry of Double Base propellant *Propellants, Explosives, Pyrotechnics* **45** pp 1-14.
[5] Beckstead M W 1993 Solid Propellant Combustion Mechanisms and Flame Structure *Pure & Appl Chem.* **65** pp 297-307.
[6] Brown R S and Jensent G E 1967 Dynamic Ballistics of Combustion Termination by Fluid Injection *AIAA Journal* **5** pp 1917-19.
[7] Aycock W C 1967 Method for Initiating or Quenching the Combustion in a Solid Propellant Rocket Misotor (United States Patent S) Patent 3,354,647.
[8] Jaroudi R and Mcdonalot A J 1964 Injection Thrust Termination and Modulation in Solid Rockets *AIAA Journal* **2** pp 2036-38.
[9] Yin J, Wu X, Su G, Zhang B, and Wangt K Experimental 1993 Study on Liquid Quench of Solid Rocket Motor *Journal of Propulsion and Power* **9** pp 719-24.
[10] Timnat Y M 1987 *Advanced Chemical Rocket Propulsion* (Haifa: Academic Press INC.) chapter 4 p 78.
[11] Tahsini A M and Farshchi M 2007 Rapid Depressurization Dynamics of Solid Propellant Rocket Motors *43rd AIAA/ASME/SAE/ASEE Joint Propulsion Conf. & Exhibit.*
[12] Jensen G E and Brown R S 1971 An Experimental Investigation of Rapid Depressurization Extinguishment *AIAA Journal* **9** pp 1667-72.
[13] Shan Y Y and Tao C C 1979 Study on Combustion Termination of Solid Propellants by Rapid Depressurization *Journal of Spacecraft and Rockets* **16** pp 353-54.
[14] Steinz A and Selizer H 1971 Depressurization Extinguishment of Composite Solid Propellants: Flame Structure, Surface Characteristics, and Restart Capability *Combustion Science and Technology* **3** pp 25-36.
[15] Lee J, Kim Y S, Baek S J and Jeong H S 2020 Study of Separation Mechanism and Characteristics of Ridge-Cut Explosive Bolts Using Numerical Analysis *International Journal of Aeronautical and Space Science* **22** pp 84-93.
[16] Kurkoski W J 2010 Pyrotechnic Valve: Design Process and Lessons Learned *46th AIAA/ASME/SAE/ASEE Joint Propulsion Conference & Exhibit* Nashville pp 1-12.
[17] Hill P G and Peterson C R 1992 *Mechanics and Thermodynamics of Propulsion second edition* **(**Addison-Wesley Publishing Company) chapter 12 p 600.
[18] Burch B T 2014 *Determining and mitigating the effects of firing a linear shaped charge under water* (Masters Theses: Missouri University of Science and Technology) chapter 1 pp 1-3.
[19] Zhang Z X 2016 *Rock Fracture and Blasting* (NORWAY: Butterworth-Heinemann) chapter 25 pp 483-90 .
[20] Sampson R Gand Peters A P 1965 Status Report Rn 120-Inch Motor Design And Development *American institute of Aeronautics and Astronautics* California pp 1-9.

[21] Phelps K L 2016 *Material properties affecting the penetration of metal targets by copper linear shaped charges* (Masters Theses: Missouri University of Science and Technology) chapter 2 p 10.
[22] Arnold W and Graswald M 2010 Shaped Charge Jet Initiation of High Explosives equipped with an Explosive Train *Insensitive Munitions & Energetic Materials Technology Symposium* Munich pp 1- 10.
[23] El-Naggar M, Belal H and Abdalla H M 2020 Experimental Investigation of Star Grains in Dual Thrust Solid Propellant Motors *Materials Science and Engineering* Cairo pp 1-18.
[24] Adel H, Ahmed M Y, Khalil M Sand Belal H M 2022 Investigation of Production Tolerances in Solid Propellant Tubular Grains *AIAA AVIATION 2022 Forum* Chicago pp 1-13.
[25] Barrere M 1960 *Rocket Propulsion* (Paris: Elsevier Publishing Company) chapter 5 p 239.
[26] John J E 2006 *Gas Dynamics* (Michigan Pearson Education International) chapter 3 pp 75-6.
[27] Krier H 1972 Solid Propellant Burning Rate During A Pressure Transient *Combustion Science and Technology* **5** pp 69-73.